https://doi.org/10.1016/j.scitotenv.2023.168316

Origin and transformation of volatile organic compounds at a regional background site in Hong Kong: Varied photochemical processes from different source regions

Qi Yuan[1], Zhuozhi Zhang[1], Yi Chen[2], Lirong Hui[3], Meng Wang[1], Men Xia[1,6], Zhouxing Zou[1], Wan Wei[1], Kin Fai Ho[4], Zhe Wang[3], Senchao Lai[5], Yingyi Zhang[5], Tao Wang[1], Shuncheng Lee[1*]

[1] *Department of Civil and Environmental Engineering, The Hong Kong Polytechnic University, Hong Kong SAR, 999077, China*

[2] *Department of Chemistry, The Hong Kong University of Science and Technology, Hong Kong SAR, 999077, China*

[3] *Division of Environment and Sustainability, The Hong Kong University of Science and Technology, Hong Kong SAR, 999077, China*

[4] *School of Public Health and Primary Care, The Chinese University of Hong Kong, Hong Kong SAR, 999077, China*

[5] *School of Environment and Energy, South China University of Technology, Guangzhou 510006, China*

[6] *Institute for Atmospheric and Earth System Research, Faculty of Science, University of Helsinki, Helsinki 00014, Finland*

[*]To Whom Correspondence Should be addressed

E-mail: shun-cheng.lee@polyu.edu.hk

Tel: +852 27666011

Abstract

Volatile organic compounds (VOCs) are important gaseous constituents in the troposphere, impacting local and regional air quality, human health, and climate. Oxidation of VOCs, with the participation of nitrogen oxides (NO_x), leads to the formation of tropospheric ozone (O_3). Accurately apportioning the emission sources and transformation processes of ambient VOCs, and effectively estimation of OH reactivity and ozone formation potential (OFP) will play an important role in reducing O_3 pollution in the atmosphere and improving public health. In this study, field measurements were conducted at a regional background site (Hok Tsui; HT) in Hong Kong from October to November 2020 with proton-transfer-reaction time-of-flight mass spectrometry (PTR-ToF-MS). VOC data coupled with air mass back trajectory cluster analysis and receptor modelling were applied to reveal the pollution pattern, emission sources and transformation of ambient VOCs at HT in autumn 2020. Seven sources were identified by positive matrix factorization (PMF) analysis, namely vehicular + industrial, solvent usage, primary oxygenated VOCs (OVOCs), secondary OVOCs 1, secondary OVOCs 2 (aged), biogenic emissions, and background + biomass burning. Secondary formation and vehicular + industrial emissions are the vital sources of ambient VOCs at HT supersite, contributing to 20.8% and 46.7% of total VOC mixing ratios, respectively. Integrated with backward trajectory analysis and correlations of VOCs with their oxidation products, short-range transport of air masses from inland regions of southeast China brought high levels of total VOCs but longer-range transport of air masses brought more secondary OVOCs in aged air masses.

Photolysis of OVOCs was the most important contributor to OH reactivity and OFP, among which aldehyde was the dominant contributor. The results of this study highlight the photochemical processing of VOCs from different source regions which should be considered in strategy making for pollution reduction.

1. Introduction

Volatile organic compounds (VOCs) are photochemically reactive organic species with high vapor pressure in the atmosphere. VOCs play crucial roles in atmospheric chemistry because they are precursors of secondary organic aerosol (SOA) (Seinfeld and Pandis, 2016) and tropospheric ozone (O_3) (Atkinson, 2000;Atkinson and Arey, 2003), and can also affect the oxidation capacity of the atmosphere (Mohd Hanif et al., 2021). In addition, VOCs and their oxidation products pose health risks to humans due to their toxic nature (Jerrett et al., 2009;St Helen et al., 2014).

VOCs can be emitted from anthropogenic sources (e.g., vehicle exhaust, industrial material and processes, and solvent usage), and biogenic (e.g., plant growth and tree leaves) sources (Wei et al., 2011;Tsui et al., 2009;Mo et al., 2016). Oxygenated VOCs (OVOCs) are also an important category of VOCs, which mainly compose of aldehydes, ketones, alcohols, and acids. OVOCs not only can be emitted from common biogenic and anthropogenic sources but also be formed via atmospheric oxidation processes. Due to complex emission sources and sinks, the ambient levels of OVOCs and their sources were important but not well quantified (Millet et al., 2010). Most previous studies on VOCs were conducted in urban and rural areas. Generally, vehicle exhaust and solvent

usage are the biggest sources of VOCs in these urban areas with high populations (Yang et al., 2022;Li et al., 2022;Zhou et al., 2019). While in rural areas, biogenic sources and biomass burning are also important sources depending on local emissions or atmospheric transportation (Salvador et al., 2021;Han et al., 2019b). Due to the limited local pollution sources, the atmospheric VOCs in remote or background sites are greatly influenced by the transport of air masses from surrounding polluted areas (Mohd Hanif et al., 2021). Nevertheless, the relative contributions of local biogenic and anthropogenic emissions are still important contributors to VOCs in remote sites (Legreid et al., 2007;Xu et al., 2022;Baudic et al., 2016). The diversity of sources of VOCs in the regional background atmosphere was not well understood, let alone the impact on the atmospheric reactivity. Research on the VOC characteristics of background sites would provide a scientific basis for better understanding the VOCs and the transportation of air pollutants in regions, which has significant implications for air pollution control.

Pearl river delta (PRD) is one of the fastest-growing urban agglomeration in China with frequent high O_3 levels. Although many air pollution control strategies have been applied to diminish the ozone precursors locally, the increasing O_3 trend and regional photochemical smog problem remains (Cao et al., 2024). Only a few numbers of studies on VOCs with limited OVOC species were carried out in the field campaigns at background sites in the PRD region (Tan et al., 2021;Xue et al., 2016;Li et al., 2018). Thus, it is of great of great importance to conduct comprehensive measurement of OVOCs for regional environmental quality assessment and environmental pollution

trend prediction. The present study is based on ambient measurements of VOCs using proton-transfer-reaction time-of-flight mass spectrometry (PTR-ToF-MS) at a regional background site of Hong Kong during the autumn period of 2020. The primary objective of this study is to investigate the role of different sources in the variations of VOCs. Source apportionment and regional contributions were investigated based on the PMF model as well as back trajectory analysis. Information about OH reactivity and OFP were assigned to resolved sources and clusters, indicating the emission reduction at different stages of pollution.

2. Measurements and Methods

2.1.Sampling site and meteorology

To investigate the pollution characteristics of VOCs in the PRD region, we conducted a field measurement on VOCs in Hong Kong as a case. In this study, the observation campaign was conducted at a coastal site in Hok Tsui (HT, **Figure S1**), Hong Kong from 7 October to 18 November 2020. The site is located at the south-eastern tip of Hong Kong Island (22.217°N, 114.25°E, 60 m above sea level), on a cliff facing the South China Sea. There is no direct stationary source nearby, and the major roads are far away from the site. Most of the time in autumn, the station receives outflow of air including polluted plumes from Hong Kong and other PRD regions, and aged continental air transported from southern and eastern China (Xue et al., 2016). Usually, it is considered as a background monitoring station, the air quality at which can well reflect the regional pollution of the PRD region.

2.2.Measurement of VOCs

A commercially available PTR-ToF-MS instrument (PTR-QiTOF-MS, IONICON Analytik GmbH, Innsbruck, Austria) was used in this study to measure VOCs and OVOCs (Text S1). Ambient air was continuously pumped with an external blower (3.0 L/min) through a 4 m long Teflon tubing (1/2'') into the room where PTR-ToF-MS located. A bypass of this 1/2'' Teflon tubing was introduced in PTR-ToF-MS for sampling. An in-line particulate filter (4.7 mm Teflon-membrane filter, Whatman Ihc. Clifton, NJ, USA) was used to prevent particles from entering the instrument. Periodic replacement of the filter was performed to maintain a relatively small impact of the particles on the inlet pressure.

Calibration of PTR-ToF-MS was performed each week with a liquid calibration unit (LCU, Ionicon) and certified standard gas mixtures (Linde Spectra Environmental Gases, USA). The gas standards contained about 1 ppm of each component, 12 of which were chosen for determining the transmission curve of the instrument and the sensitivities of those corresponding species (Table S1). Sensitivities of the uncalibrated VOC species were determined based on the empirical reaction kinetics of the PTR-ToF-MS (Yuan et al., 2017). The instrumental background signals were determined with zero air every day and subtracted from the total signals to determine the mixing ratios of VOCs and OVOCs.

2.3. Measurements of other parameters

NO, NO_2, O_3, and CO and meteorological parameters were simultaneously measured. NO and NO_2 were measured with a chemiluminescence analyzer (TEI, model 42i) with a selective blue light converter (Xu et al., 2013); O_3 was measured by a commercial ultraviolet photometric instrument (TEI, model 49i); CO was measured with a gas filter correlation analyzer (Teledyne, T300). Detailed calibration procedures were described in previous studies (Xue et al., 2016). Photolysis frequency of NO_2 (jNO_2) was measured with a MetCon Filter Radiometer. Temperature, relative humidity (RH), wind speed, and wind direction were monitored by the Hong Kong Environmental Protection Department.

2.4.Source apportionment method

Source apportionment of VOCs was performed using the positive matrix factorization (PMF) receptor model implemented within the multilinear engine (Paatero, 1999). The model configuration and post-analysis were performed with the Source Finder (SoFi, Version 6.9) tool kit for Igor Pro (Wavemetrics, Inc., Portland, Version 6.37) (Canonaco et al., 2013). In this study, 41 representative marker species with relatively higher concentrations and impact on air quality were selected and applied to identify the possible sources of VOCs in Hong Kong. The uncertainties of corresponding species were calculated from the method detection limit (MDL) and the determination error fraction, which is recommended by the user guide (Canonaco et al., 2013). Detailed information about the operation principle is described in Text S2. Two to ten factors were investigated with PMF model in robust unconstrained mode. The

optimized result was obtained with seven factors in consideration of the Q values and physical plausibility. The detailed PMF performance is exhibited in Text S3 and **Figure S2**.

2.5.Calculation of OH reactivity and OFP

The influence of VOCs on OH and ozone were determined by the VOC reaction rate with OH radical and the ozone formation potential (OFP). OH reactivity of VOCs was estimated to investigate their potential oxidation ability with OH radical by the following equation:

$$total\ OH\ reactivity = \sum k_{VOC_i+OH}[VOC_i] \quad (2)$$

where k_{VOC_i+OH} refers to the first-order rate coefficient for the reaction between VOC_i and OH radicals, $[VOC_i]$ is the measured mixing ratio of VOC_i. Reaction rate coefficients were referred from Atkinson et al. (2006), Barnes et al. (2010) and the NIST chemical kinetics database (kinetics.nist.gov/kinetics).

For a VOC species i, its OFP can be calculated as follows:

$$OFP_i = [VOC_i] \times MIR_i \quad (3)$$

In the formula, MIR_i represents the maximum incremental reactivity (MIR (gO_3/gVOC)) of each VOC species, which is derived from existing studies (Carter, 1994). $[VOC_i]$ is the ambient VOC mixing ratio (ppb) measured by PTR-MS. The unit of MIR based on mass concentration was converted to that based on VMR ($ppbO_3$/ppbVOC) and then multiplied by mixing ratio of VOC to obtain OFP (ppb).

2.6.Backward trajectory analysis

Backward trajectory analysis along with cluster analysis have been commonly used in studies of understanding VOCs source transport (Li et al., 2018;Xu et al., 2022). To track the transmission of air masses arriving at HT, the 72-h backward trajectory of air masses was computed and clustered during the sampling period using the TrajStat analysis software developed by Wang et al. (2009). The starting time was set at 0:00 local time (LT) and the arrival heights of the trajectories were 100 m above the ground. To calculate the back trajectories during the observation period, the data of Global Data Assimilation System (GDAS) with gridded resolution of 1° × 1° were downloaded from National Weather Service's National Center for Environmental Prediction (NCEP) (ftp://arlftp.arlhq.noaa.gov./pub/archives/gdas1). The hourly Backward trajectories were clustered according to their angles in the TrajStat software to analyze origins of the transported air masses arriving at HT over the observation period.

As shown in **Figure S3**, the back trajectories of air masses arriving at HT was classified into three groups. Cluster 1 accounted for 56.8% of the backward trajectories, representing slow and short-range transport of air masses that predominantly originated from inland regions of southern and eastern China. Cluster 2 accounted for 18.4% of the backward trajectories, representing coastal air masses that predominantly originated from the eastern China. Cluster 3 accounting for 24.8% of the backward trajectories, representing fast and long-range transportation of continental air masses that mainly originated from eastern and northern China.

3. Results and Discussion

3.1. Mixing ratios of VOCs

As shown in **Figure 1**, mixing ratios of various species and meteorological parameters all exhibited strong variations during the campaign. The summed mixing ratio of total VOCs varied between 9.65–140.71 ppb with an average of 33.22 ± 15.82 ppb. Ozone mixing ratios varied in the range of 14.2-174.0 ppb with an average of 49.7 ± 15.9 ppb. The average mixing ratio of NO_x was 4.1 ± 2.6 ppb. Daily mean temperature was 24.0 ± 1.8℃ with a range of 19.5 – 30.7℃. Daily mean value of RH varied between 39.8% – 96.0% with an average of 73.1% ± 10.5%. VOCs, O_3 and NO_x showed extremely high concentrations during 6 to 7 November 2020, which was caused by the typhoon off the east coast of Hong Kong. Under the influence of typhoon periphery downdraft, dramatic changes in wind direction with low wind speed and relative high temperature were observed (Figures 1(a) and 1(b)). This meteorological condition was proven to lead to adverse diffusion conditions, causing a detrimental impact on the generation, transportation and diffusion of air pollutants, causing hazy weather (Chen et al., 2023).

The average mixing ratios of ions detected by PTR-ToF-MS are listed in **Table S2**. 92 protonated ion peaks were observed in the mass spectra during the field campaign, including 84 VOC species and 8 fragments/ charge transfer ions. Based on the structures and oxygen numbers, the detected VOCs were classified into 5 categories, i.e., aliphatic hydrocarbons (HCs), aromatics HCs, $C_xH_yO_1$, $C_xH_yO_2$, $C_xH_yO_{\geq 3}$, and N-containing species. Among those categories, $C_xH_yO_1$ contributed to 53.7% of the mixing ratio of

TVOCs. $C_xH_yO_2$ and $C_xH_yO_{\geq 3}$ contributed 23.9% and 4.6% of the total mixing ratio of VOCs. Aliphatic and aromatic HCs had molar contributions of 8.5% and 4.9% of measured TVOC mixing ratios, respectively. N-containing species only contributed to 4.4% of measured TVOC mixing ratios. OVOCs can be directly emitted from both anthropogenic and biogenic sources (Placet et al., 2000;Sawyer et al., 2000;Fall, 1999), and largely derived from secondary formation (Atkinson, 2000). Yuan et al. (2012) observed photochemical losses of HCs and secondary formation of a large proportion of carbonyls in rural and suburban PRD. Despite the fact that PTR-ToF-MS with H_3O^+ chemistry may be available to quantify only limited species of some alkenes and aromatics, relatively high proportion of OVOCs (81.2%) than HCs in this coastal background site indicated more secondary formation from oxidation of VOCs.

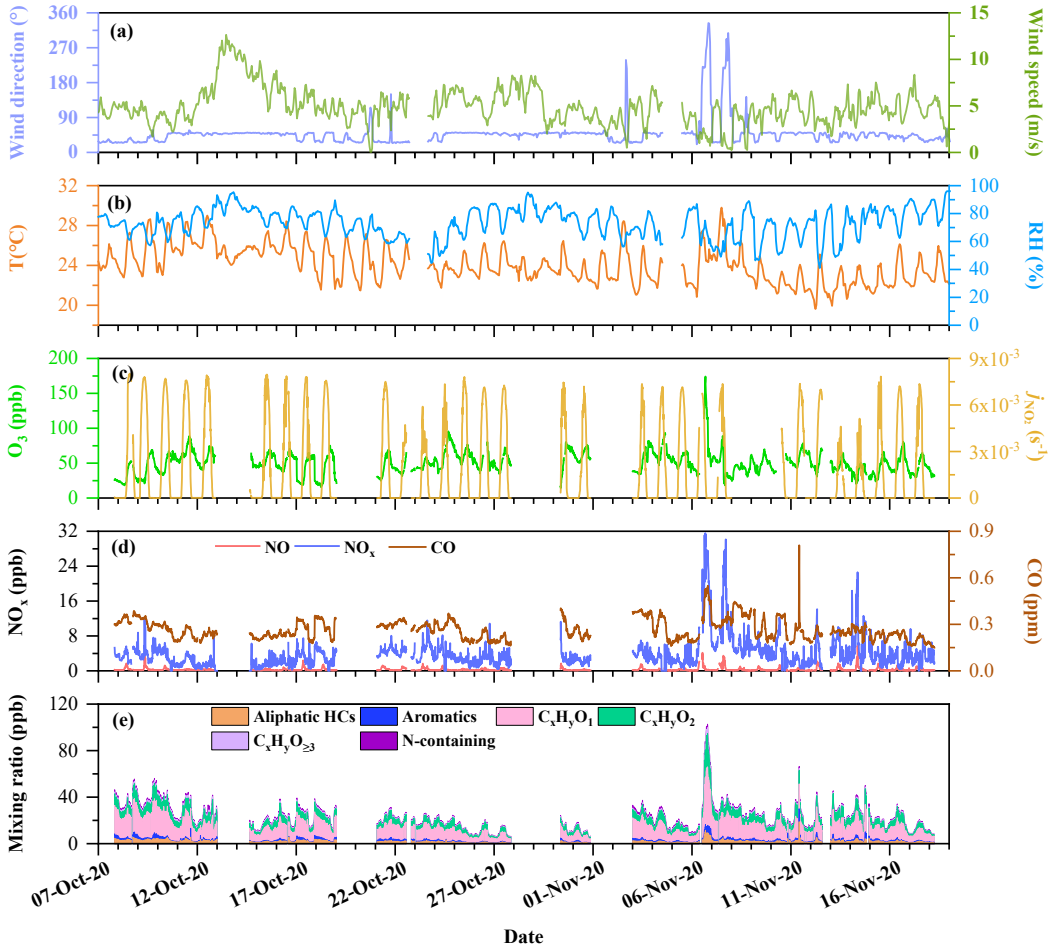

238

239 **Figure 1.** Time series of air pollutants and meteorological parameters observed at HT

240 from 7 October to 18 November 2020. The breaks of data sets were due to typhoon

241 and calibration and maintenance of the instruments.

The top 10 VOCs measured during the campaign were methanol (4.63 ± 2.47 ppb), acetone (3.37 ± 1.55 ppb), acetic acid (2.51 ± 1.58 ppb), acetaldehyde (1.72 ± 0.88 ppb), formaldehyde (0.93 ± 0.39 ppb), formic acid (0.87 ± 0.47 ppb), methyl acetate (0.82 ± 0.48 ppb), butentes (0.61 ± 0.42 ppb), butyric acid (0.41 ± 0.33 ppb), and acetonitrile (0.41 ± 0.26 ppb), contributing to 70% of the total mixing ratio of detected VOCs (**Figure 2**). In aromatic category, which is widely recognized to be emitted from anthropogenic sources, toluene (0.39 ± 0.35 ppb) is the most abundant species, followed by C_8 aromatics (0.31 ± 0.36 ppb) and benzene (0.27 ± 0.15 ppb) (Table S2). Isoprene and monoterpene are emitted from biogenic sources, which have average values of 0.20 ± 0.18 ppb and 0.04 ± 0.09 ppb, respectively (Table S2).

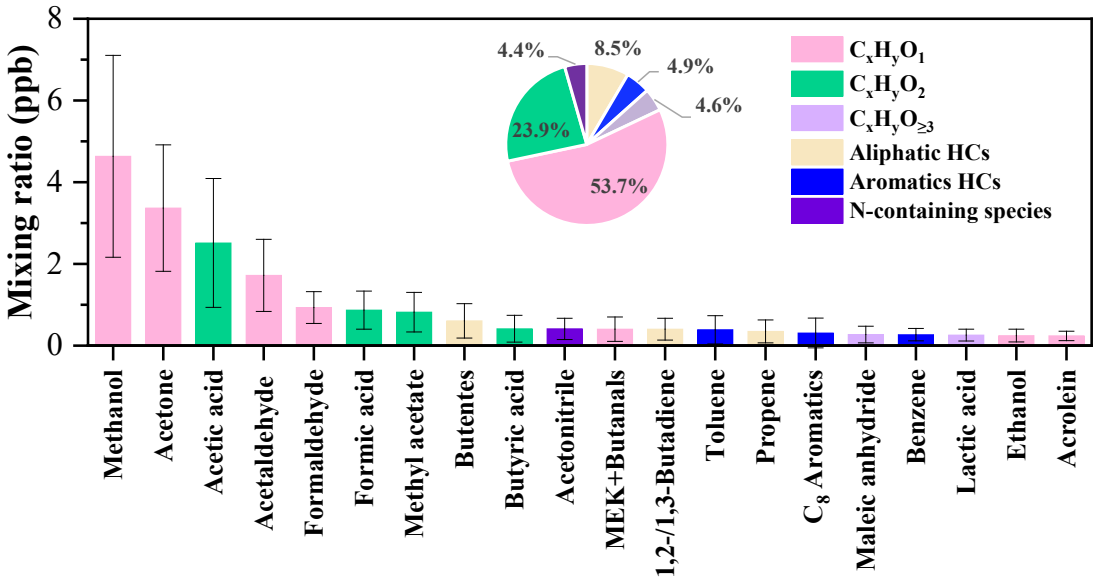

Figure 2. Top 20 Species of VOCs and the relative contribution of six chemical classes of VOCs.

To assess the pollution levels of VOCs at background Hong Kong, their averaged mixing ratios in this study were compared with those in other background (Tan et al.,

2021;Li et al., 2018;Huang et al., 2019;Shao et al., 2020;Xue et al., 2013;Debevec et al., 2017;Legreid et al., 2007;Xu et al., 2022), rural (Han et al., 2019b;Jordan et al., 2009) and urban sites (Huang et al., 2015;Han et al., 2023;Cui et al., 2021;Li et al., 2022;Zhu et al., 2019;Liu et al., 2015;Huang et al., 2020) (Table 1). Large differences in the mixing ratio levels of VOCs were found at different sites. Generally, the selected VOCs were similar to some urban background and regional sites (e.g., Nanling and Nan'ao), several times higher than those remote background sites, e.g., Nam Co and Cyprus, and much lower than those in most of the urban areas. Isoprene and monoterpenes are mainly emitted from biogenic sources. Equivalent levels of isoprene were found in this study with background Guangdong and roadside Hong Kong, possibly due to the similar vegetation type and coverage. Emission from vehicles may also contribute to isoprene in roadside environment (Borbon et al., 2001). The difference of isoprene mixing ratio between this study and previous studies at HT was caused by the temperature and solar dependance of isoprene, which will be discussed in Section 3.3. MVK+MACR are first generation oxidation products of isoprene under high NO_x conditions. Mixing ratio of MVK+MACR lied in a moderate queue between the lower values in remote background sites and higher values in urban environments, which reflected the certain impact of anthropogenic activities. Aromatic HCs are mainly emitted from anthropogenic sources, e.g., solvent usage, industrial and vehicular emissions (Yang et al., 2022). Stable pollution levels of BTEX (sum of benzene, toluene and C_8 aromatics) were found at HT in autumn from 2012 to 2020 with average mixing ratio around 1 ppb, lower than most of the urban background and urban sites.

Particularly, benzene at HT was comparable with those in other background and urban sites, but toluene and C_8 aromatics were lower than those reported in other background and urban sites. Due to the relatively higher reactivity and the different source or source regions, the variance in mixing ratios of toluene and C_8 aromatics would be caused by photochemical oxidation during the transportation of pollutants .

As the most abundant OVOC detected in this study, methanol is higher than background Guangzhou and rural site in Shenzhen, and was around 2-5 times lower than those in urban sites (Han et al., 2019a). Previous studies reported methanol in urban PRD are dominantly from anthropogenic sources (Zhu et al., 2019;Han et al., 2019a). Higher mixing ratios of acetaldehyde and acetone were found in this study than those in other background and rural sites, and even urban roadside Hong Kong (Cui et al., 2021). Known sources of acetaldehyde include anthropogenic emissions (e.g., mobile sources and stationary combustion), biogenic emissions (i.e., decaying plants), biomass burning and seawater (Millet et al., 2010). Meanwhile, another vitally important source of acetaldehyde is degradation of non-methane VOCs such as $>C_3$ alkanes, $>C_2$ alkenes and ethane (Fischer et al., 2014). Acetone levels in the troposphere are strongly associated with anthropogenic sources in both primary emissions and secondary production from oxidation of anthropogenic HCs (Moore et al., 2012;Singh et al., 1994). The mixing ratios of isoprene and monoterpenes were lower in this study than in previous studies at Hok Tsui, while the mixing ratio of acetaldehyde was higher than in those studies (Li et al., 2018;Tan et al., 2021) (Table 1). This implies that neither biogenic emissions nor secondary formation from biogenic VOCs were the major

contributors to acetaldehyde in this study. As there was no direct anthropogenic emission source at HT, the high mixing ratios of acetaldehyde and acetone implies that transportation and atmospheric oxidation of anthropogenic VOCs may contribute a certain amount of these OVOCs at this background site. This was also supported by the fact that higher propene and butadienes (0.348 ± 0.280 ppb and 0.402 ± 0.266 ppb), anthropogenic precursors of acetaldehyde, were observed in this study than those (0.019 ± 0.043 ppb and 0.006 ± 0.018 ppb) reported by Li et al. (2018). The overall results of the variations of VOCs and OVOCs implies that anthropogenic sources strongly influence the air quality in background Hong Kong.

3.2. Diurnal variations

Diurnal profiles of selected VOCs species are shown in **Figure 3**. Diurnal variations of VOCs are influenced by emission sources, chemical removal or formation from reactions with atmospheric oxidants, and atmospheric dynamic (Prévôt et al., 2000). Emission of terrestrial plants of isoprene and monoterpenes has dependency on temperature and solar radiation (Singsaas and Sharkey, 1998;Tingey et al., 1980). With higher temperature, mixing ratios of isoprene and monoterpenes are higher during 7-13 October and 6-7 November 2020 (Figure S4). With the increasing temperature and solar radiation, clear diurnal pattern with mixing ratios increasing directly after sunrise and reaching maximum at noon was observed (Figure S5). MVK and MACR, showed common diurnal cycles of photooxidation products with maxima occurring in the daytime (Figure 3). Acetonitrile is widely considered a tracer for biomass burning and

is known as a long-lasting species with an atmospheric lifetime of approximately six months (de Gouw et al., 2003;Singh et al., 2003). The mixing ratio of acetonitrile remained relatively stable during the day (Figure 3), while high levels of acetonitrile were found only on 12 October 2020 (Figure S4). This indicated the less contribution of biomass burning sources.

Diurnal patterns of HCs from anthropogenic sources, e.g., propene and aromatics (Figure 3), were unimodal at HT background site. The mixing ratios of propene, benzene, toluene and C_8 aromatics started to decrease during the daytime, then increased after sunset and reached the highest in the morning. In some urban areas, diurnal cycles of aromatic HCs show bimodal patterns with a morning and an evening peak due to the traffic emissions (Li and Wang, 2012). The different diurnal patterns of aromatics in this study from those in urban areas suggest significant contributions from regional transport rather than local traffic emissions. Furthermore, meteorological conditions and chemical processes are responsible for the diurnal variation of these anthropogenic VOCs. Yang et al. (2013) reported diurnal variation of long-term planetary boundary layer (PBL) height at Hong Kong, that is, the PBL height grows rapidly in the morning hours, achieves maximum value in the afternoon, and decays in the late afternoon. The increase of PBL in the afternoon facilitates the dispersion of the primarily emitted VOCs, and the decrease of PBL in the late afternoon till the morning led to the accumulation of the VOCs (Sun et al., 2021). On the other hand, the high reaction rate coefficient of propene (2.6×10^{-11} cm^3 $molecule^{-1}$ s^{-1}) and aromatic HCs with OH ($(1.22 – 23.1) \times 10^{-11}$ cm^3 $molecule^{-1}$ s^{-1}) with OH radical led to their fast

346 depletion in the daytime, which is in line with the strong solar radiation, and high
347 mixing ratio of O_3 (Figure S5) (He et al., 2022;He et al., 2023).

348 OVOCs can not only be primarily emitted from anthropogenic and biogenic sources,
349 but also secondarily formed from the oxidation of HCs. Methanol and methyl acetate
350 both showed two peaks during the rush hours and in the afternoon (Figure 3),
351 respectively, indicating the contributions of both primary emissions and secondary
352 formation. The diurnal profiles of phenol exhibited a significant upward trend with
353 maxima occurring between 10:00-14:00 during the daytime, in accordance with the fact
354 that they are early generation photooxidation products of aromatic HCs (Calvert et al.,
355 2002). Benzoic acid, known as a later generation product from oxidation of aromatics
356 (Calvert et al., 2002), showed a deferred peak compared to phenol and cresol, which
357 reflected the ageing of the air at this background site. Formaldehyde, acetone,
358 acetaldehyde, and acetic acids in the troposphere are strongly influenced by the
359 oxidation of HCs (Khan et al., 2015;Fortems-Cheiney et al., 2012;Millet et al.,
360 2010;Paulot et al., 2011). Together with higher temperature, jNO_2 and O_3 (Figure S5),
361 these OVOCs showed clear daytime peaks, indicating that photochemical processes
362 play a substantial role at this coastal background site.

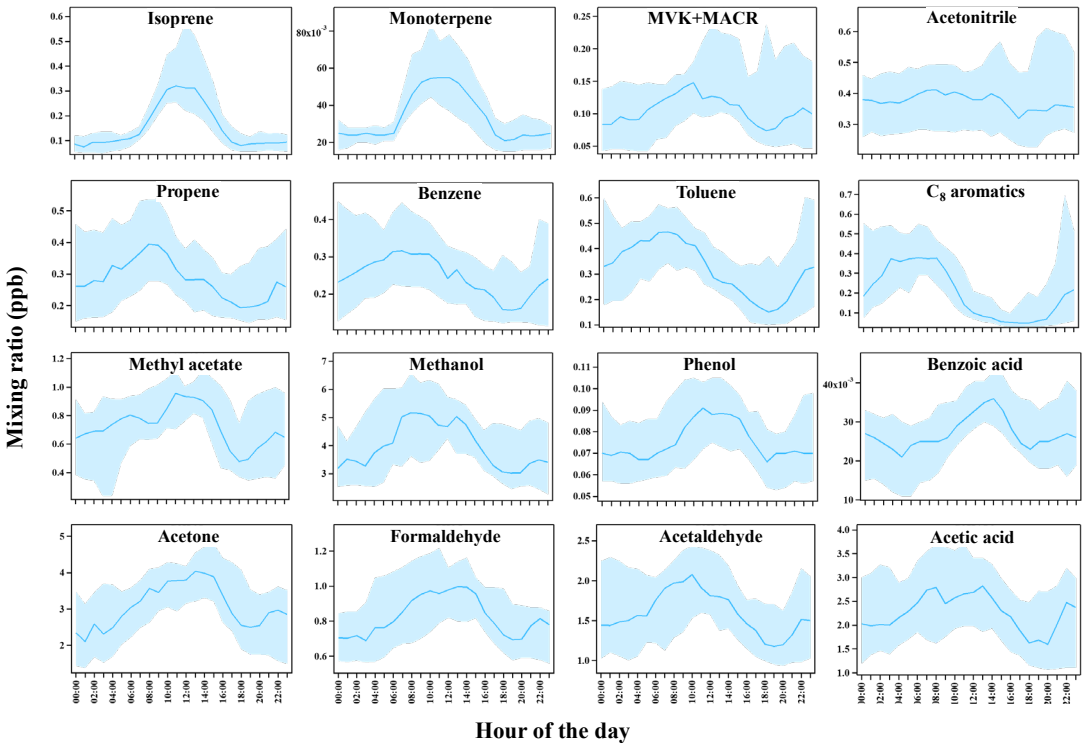

Figure 3. Diurnal variations in the mixing ratios of typical VOCs at HT site HT during 7 October to 18 November 2020.

3.3 Atmospheric processing of VOCs during regional transport

As discussed in Section 3.1 and 3.2, considerable levels of anthropogenic VOCs and their oxidation processes with substantial OVOC formation were observed at this background site. Under the influence of Asian monsoon during the autumn, this site receives air masses mainly from eastern and northern China with polluted plumes. To corroborate this atmospheric process during regional transport, here we show the results of mixing ratios, day to night (D/N) ratios, and correlations of paired precursor VOCs and OVOCs in three clusters of air masses from different origins.

In Table S3, total VOCs and NO_x showed decreased mixing ratios, while O_3 increased from short-range transport (Cluster 1) to coastal air masses (Cluster 2) and long-range

377 transport (Cluster 3). The reduction of VOCs and NO_x may be due to (1) different
378 emission sources in the source regions brought different levels of pollutants, (2)
379 diffusion of air during the transportation along with the air masses, (3) photooxidation
380 of VOCs and NO_x during the transportation of air masses as the distance increased.
381 Meanwhile, the increasing of O_3 from Cluster 1 to 3 was also observed in a previous
382 study at HT (Li et al., 2018), indicating that the photochemical loss of primarily emitted
383 VOCs were transferred to secondary products with higher reactivity, enhancing the O_3
384 pollution. As shown in Figure S6, the D/N ratios of $C_xH_yO_1$, $C_xH_yO_2$ in the whole
385 sampling period were higher than 1.0, which confirmed the secondary formation under
386 photooxidation. Despite that mixing ratios of most VOCs are highest in Cluster 1, the
387 D/N ratios of OVOCs were mostly higher in Cluster 2 and 3, indicating air masses were
388 more aged during the regional transport.

389 Acetic acid is among the most abundant and ubiquitous trace gases in the atmosphere
390 (Paulot et al., 2011;Millet et al., 2010). While direct sources including emissions from
391 anthropogenic sources, vegetation, soil and biomass burning do have contributions, the
392 OH oxidation of acetaldehyde represents an more important source of atmospheric
393 acetic acid (Paulot et al., 2011). Acetaldehyde is mainly produced from oxidation of
394 primary nonmethane VOCs, e.g., isoprene, terpenes, acetone, $>C_2$ alkenes, ethanol,
395 methylglyoxal and MEK (Fischer et al., 2014). Thus, the relationship among precursors,
396 acetaldehyde and acetic acid could provide insight into the photochemical activities and
397 oxidation states of air from regional transport. In this study, the sum of detected propene,
398 cyclobutadiene, butadiene, butentes, ethanol and methylglyoxal were selected as

399 anthropogenic precursor of acetaldehyde to investigate the ageing process during the
400 transport of air masses arriving at HT. The sum of the precursors showed strong
401 correlation with acetaldehyde (R^2=0.894-0.918, $p<0.05$) and acetic acid (R^2=0.762-
402 0.843, $p<0.05$) in three clusters (Figure 4), which indicated the anthropogenic sources
403 from continental regions is a major contributor to acetaldehyde and acetic acid. The
404 slopes between precursors with acetaldehyde and acetic acid were higher in Cluster 2
405 and 3 than Cluster 1, suggesting stronger photochemical formation of acetaldehyde and
406 acetic acid from lower levels of these anthropogenic precursors in air masses
407 transported from longer distance.

408 As mentioned above, aromatic HCs mainly come from vehicle and industrial
409 emissions, solvent usage, and other anthropogenic sources. The major sink of aromatics
410 in the atmosphere is the reaction with OH, forming multi-generation products in
411 sequence. For instance, phenol, cresols, methylbenzaldehyde are typical first-
412 generation ring-retaining products of benzene, toluene and xylenes, whilst benzoic acid,
413 nitrophenol, and methylbenzoyl acids are the later generations. In this study, phenol,
414 benzaldehyde, cresols, methylbenzaldehyde, C_2-phenols, trimethylphenols and
415 methylchanicol were summed up as first-generation products of aromatics. Similar to
416 the relationship between precursors with acetaldehyde and acetic acid, total aromatics
417 exhibited strong positive correlations with total oxygenated aromatics in the three
418 clusters (R^2= 0.662-0.805, $p<0.01$), with higher slopes in Cluster 2 and 3 other than
419 Cluster 1. Given that benzaldehyde is one of the first-generation products of toluene,
420 better correlations with higher slopes were found in Cluster 2 and 3 than in Cluster 1.

The significant positive correlations of these paired precursors and products confirmed the transformation of primarily emitted VOCs to oxygenated products during the regional transport, especially in the air masses from far away. These oxygenated products with higher reactivity may further influence the formation of O_3 and SOA. We highlight that although the short-range transport with lower diffusion brings high levels of pollutants, the enhancement of OVOCs with high reactivity during the ageing of air masses from long-range transport should not be ignored.

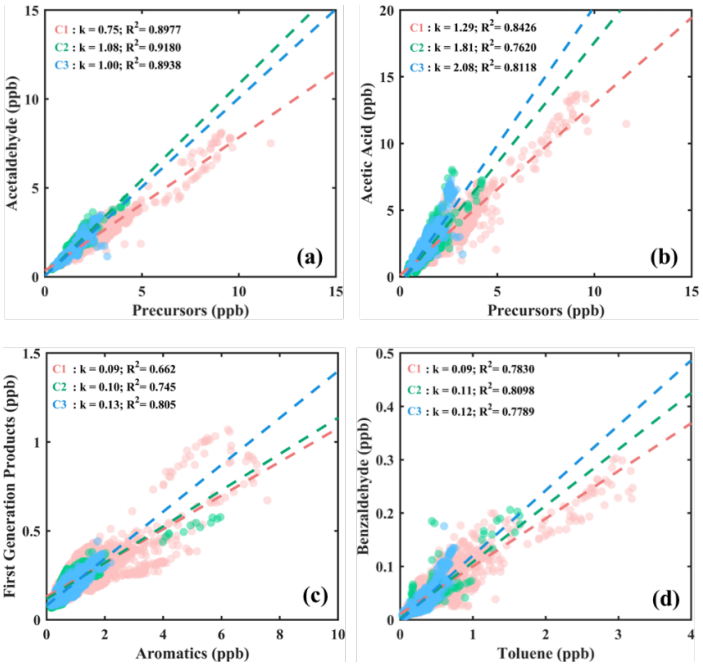

Figure 4. Correlations between (a) precursors with acetaldehyde, (b) precursors with acetic acid, (c) aromatics with their first-generation products, (d) toluene with benzaldehyde in the three clusters.

3.4. Source apportionment of VOCs

Figure 5 shows the factor profile, diurnal patterns, and relative contributions of the selected PMF solution at HT. The model represents over 83% of these selected species

436 and thus in general explains the variations of these species well. The diurnal patterns of
437 these factors illustrate that distinct differences exist in the mixing ratios, variations, and
438 source compositions of certain VOCs. In the following, we present a detailed discussion
439 of the factor characteristics of the PMF results. In this study, a solution with seven
440 factors for the PMF analysis was chosen as the optimal result. The seven factors were
441 assigned to sources of vehicle and industrial emissions (20.8%), solvent usage (10.5%),
442 primary OVOCs (13.1%), secondary OVOCs 1 (33.6%), secondary OVOCs 2 (6.7%),
443 biogenic emissions (4.3%), and background + biomass burning (10.9%) (Figures 5 and
444 6).

445 Factor 1 accounts for 27% of methanol, 33% of ethanol, 43% of propene, 30% of
446 butene, 33% of benzene, 24% of toluene and over 65% of C_8-C_{10} aromatic HCs.
447 Propene, butene, benzene and toluene are known to be emitted from vehicular traffic
448 (Nelson and Quigley, 1984;Löfgren and Petersson, 1992). Since toluene and benzene
449 are generally co-emitted from similar sources but then undergo photochemical loss at
450 differing rates, the ratios of toluene to benzene (T/B) in ambient air provide useful
451 insight to diagnose the emission sources, photochemical processes, as well as the
452 transport and dilution processes (Borbon et al., 2013;McKeen and Liu, 1993;McKeen
453 et al., 1996). Tunnel and roadside measurements indicate that the ambient T/B ratios of
454 1-2 characterized the impact of fresh vehicular emissions (Huang et al., 2015). The
455 average ratio of T/B for factor 1 was 1.05, indicating that the factor is related to vehicle
456 exhaust. Meanwhile, methanol and C_8-C_{10} aromatics are typical VOC species emitted
457 from industrial raw materials and industrial processes (Hong-li et al., 2017;Zhang et al.,

458 2013;Wang et al., 2015). Therefore, factor 1 was interpreted as a mixture of vehicle and
459 industrial activity.

460 Factor 2 was loaded on a significant amount of methyl acetate (35%), ethyl acetate
461 (42%), toluene (52%), C_8 aromatics (29%) and oxygenated aromatics with one oxygen
462 atom, e.g., benzaldehyde (58%), cresol (28%), methyl-benzaldehyde (31%). Esters is
463 abundant in the context of industrial solvent usage in PRD and in China (Ou et al.,
464 2015;Mo et al., 2016;Yang et al., 2023). Ou et al. (2015) reported that 95% of ethyl
465 acetate were emitted from solvent usage, especially in gravure printing, furniture-
466 making and shoe-making industries. Toluene and C_8 aromatics were recognized as the
467 most abundant species for solvent usage in China (Liang et al., 2017). Previous studies
468 found that the T/B ratio of industrial processes involving solvent use was higher than 3,
469 since toluene was widely used as a solvent in many industries (Huang et al., 2024). The
470 average ratio of T/B in factor 2 was 4.26, which could be referred to as solvent usage
471 related sources. Oxygenated aromatics are first generation products formed from
472 photochemical reactions of aromatic HCs (e.g., benzene and toluene) which also have
473 high reactivity with OH radicals (Gery et al., 1985;Calvert et al., 2011). The rapid
474 decrease of the contribution of solvent usage after sunrise was affected by
475 photochemical removal of aromatic HCs and early generation products of aromatics
476 (Figure 5b).

477 Factors 3, 4 and 5 were characterized by high mixing ratios of OVOCs. Factor 3
478 featured high fractions of methanol, acetaldehyde, formaldehyde, formic acid, ethanol,
479 and hexanals. Methanol and ethanol were mainly contributing from primary sources,

such as vehicle exhausts, solvent usage, volatile chemical products, and personal care products (Yeoman et al., 2020). Formaldehyde and acetaldehyde were reported to be emitted from mobile sources, printing, and stationary combustion in urban areas (Simon et al., 2010), and formic acid were mainly from industrial solvent (Ou et al., 2015). Hexanals can be released cooking emissions in ambient air (Abdullahi et al., 2013). The diurnal profile of factor 3 exhibited insignificant variability with slight increases between 7:00-11:00 and 16:00-18:00, indicating insignificant contribution from photochemical reactions. Thus, factor 3 was mainly contributed from mixing primary sources.

Factor 4 explained predominant fraction of most oxygenated compounds, i.e., over 30% of methanol, acrolein, MVK+MACR, MEK, and more than 40% of formic acid, acetone, acetic acid, and PAN, which are secondary products from photochemical reactions (Zhang et al., 2021;Abdullahi et al., 2013). The diurnal variations of factor 4 showed a clear peak in the midday, confirming that factor 4 represents OVOCs derived from secondary formation. Compared with factor 4, factor 5 contains a high proportion of oxygenated aromatics, especially those with 2-3 oxygen atoms. The diurnal profile of factor 5 has a daytime peak with the highest value at around 16:00, implying the formation of later generation products. Moreover, significant positive correlations between aromatic HCs and oxygenated aromatics were found in all the three clusters (Figure 4), suggesting that factor 5 represents OVOCs derived from ageing of the secondary OVOCs.

Factor 6 contained a particularly large content of isoprene (63%) and monoterpene (65%). Isoprene and monoterpenes are well recognized as tracers for biogenic sources since they are largely emitted from plants. The diurnal pattern exhibited a daytime peak between 6:00 – 18:00, coinciding with the temperature and solar dependency of biogenic emissions (Guenther et al., 1995). Hence factor 6 was considered to be biogenic sources.

Factor 7 contained low reactive VOCs and high acetonitrile (31%), 1,2-/1,3-butadiene (24%) and phenol (17%). The high proportion of acetonitrile is a strong indication that the factor is a combination of background and biomass burning signals. In addition, butadiene and phenol are known to exist in biomass burning plumes (Salvador et al., 2021). The diurnal pattern of factor 7 remained stable during the whole day. Thus, factor 7 was considered to be background +biomass burning.

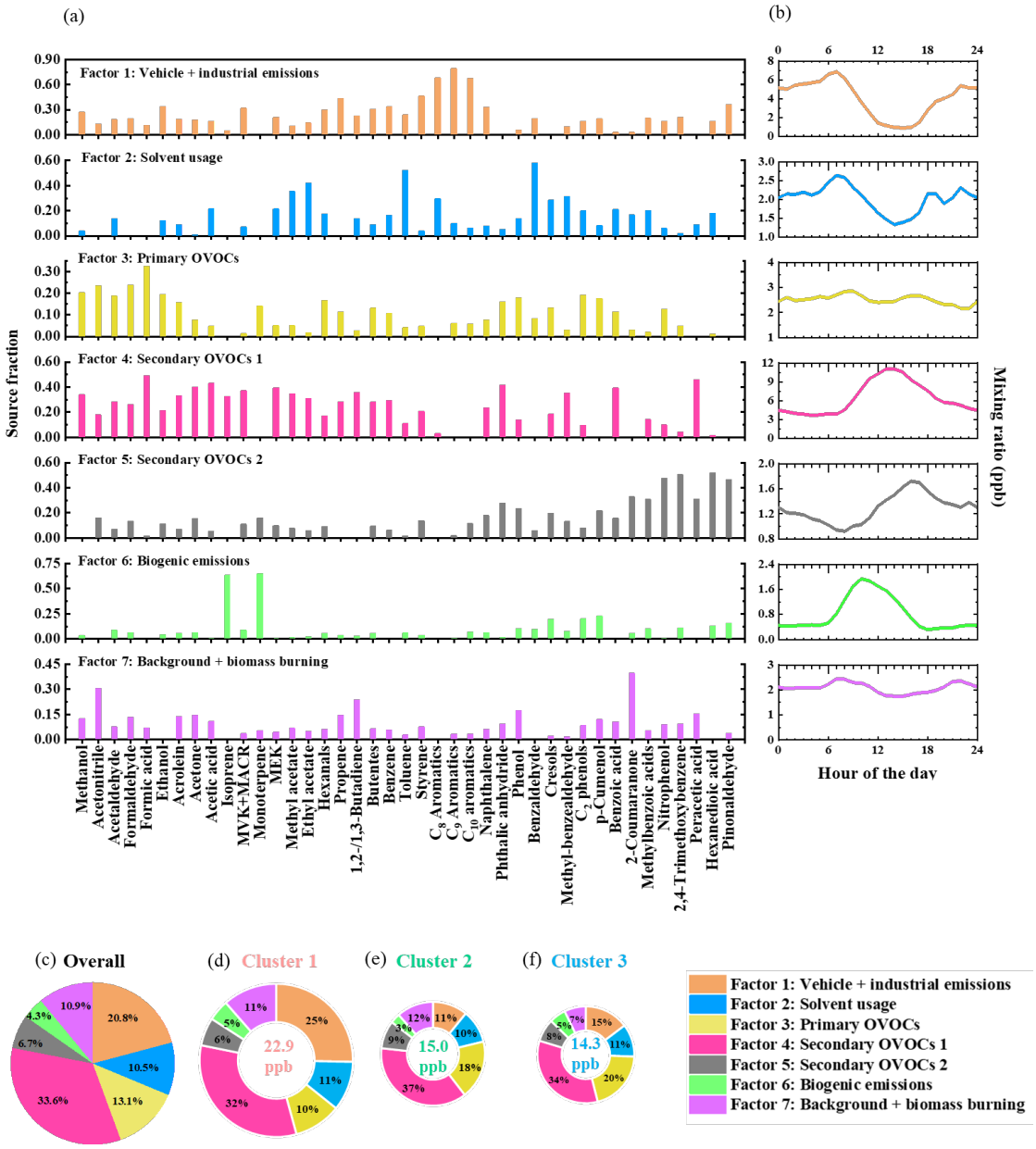

Figure 5. PMF results of VOCs at HT during 7 October to 18 November 2020, showing (a) factor profiles and (b) diurnal pattern, source contribution of each factor to VOCs in (a) the whole campaign, (b) Cluster1, (c) Cluster 2, and (d) Cluster 3.

Source contributions combined with cluster analysis were conducted in this study. The average TVOC mixing ratios in cluster 1, 2, and 3 were 22.9, 14.3, and 15.0 ppb, respectively (Figure 5 (d-f)). Contribution of the seven factors displayed strong

522 variations in the three clusters. Vehicle + industrial emissions contributed to 25% of
523 VOCs in Cluster 1, but only 15% and 11% in Clusters 2 and 3. Primary OVOCs from
524 anthropogenic sources accounted for 20% and 18% in Clusters 2 and 3, while it
525 accounted for only 10% in Cluster 1. These indicated that the distributions of VOC
526 profiles were largely affected by different primary anthropogenic sources in continental
527 regions and coastal areas. Sum of secondary OVOCs 1 and 2 contributed to 46% and
528 42% of VOCs in Cluster 3 and 2, but only 38% of VOCs in Cluster 1. Knowing that the
529 transportation distance was decreasing from cluster 3 to Cluster 1, the decrease of
530 Vehicle + industrial dominant sources and increase of secondary OVOCs implied the
531 ageing of air masses during the transport processes.
532
533 **3.5 Atmospheric oxidation capacity from different air masses**
534 In order to compare the influence of different VOCs on atmospheric chemistry and
535 photochemical production of O_3, OH reactivity and OFP were investigated along with
536 cluster analysis. The average value of total reactivity measured in this study is 5.02 s^{-1}
537 with a maximum value of 36.02 s^{-1}. Top 10 contributors of OH reactivity were shown
538 in Figure S7, many of which are emitted from anthropogenic sources. Acetaldehyde
539 contributed the most to OH reactivity with an average of 0.63 s^{-1}, followed by isoprene
540 (0.48 s^{-1}), butadiene (0.45 s^{-1}), butanedione (0.31 s^{-1}), and propene (0.22 s^{-1}). These 5
541 VOCs altogether accounted for over 46% of the total OH reactivity.
542 Figure 6(a-c) shows the contributions of 6 chemical classes to OH reactivity in the
543 three cluster and their corresponding diurnal variations. Clearly, the OH reactivity were

544 highest in Cluster 1, with an average value of 5.6 s^{-1}, compared to 3.6 s^{-1} and 3.2 s^{-1} in
545 Cluster 2 and 3. Generally, OVOCs contributed chiefly to OH reactivity (over 50%) in
546 all three clusters, followed by aliphatic HCs (>35%), aromatics (>8%) and N-containing
547 species (2%). The relative contributions of the principal groups of VOCs to OH
548 reactivity was distinct in air masses from the three regions. The contribution of OH
549 reactivity from HCs (aliphatic and aromatics) was in decreasing order (from 48% to
550 43%) from Cluster 1 to Cluster 3, while that of OVOCs was increasing (from 50% to
551 55%).

552 Diurnal variations of the OH reactivity was completely different in the three clusters.
553 In Cluster 1, the OH reactivity shows a bimodal (6:00-10:00 and 16:00-21:00 LT) with
554 a highest value (5.7 s^{-1}) at 19:00 LT, which were mainly contributed by aliphatic and
555 aromatic HCs. This should be attributed to freshly emitted urban plumes from upwind
556 to Hong Kong. In Cluster 2, the OH reactivity exhibited a broad peak from 6:00-20:00
557 LT with the highest value at 9:00 LT. This diurnal pattern arose from the emission of
558 aromatics and aliphatic HCs and then decreased from the photochemical consumption
559 of HCs and formation of OVOCs during the transport of air masses from the coastal
560 cities. In Cluster 3, $C_xH_yO_1$ and aliphatic HCs dominated the OH reactivity in a broad
561 peak between midnight and late afternoon. Except for the sharp peak at 10:00 LT which
562 was due to emission of biogenic VOCs and some aromatics during grass cutting by
563 machine on 11 October 2020, the whole peak was attributed to enhanced
564 photochemistry processes during regional transport of air masses.

565 To ascertain the contributions of different chemical classes of compound to total OFP,

566 the OFP estimated from detected VOCs in this study in the three clusters are shown in
567 Figure 6(d-f). The overall value of OFP during the whole sampling period is 73.6 ± 42.3
568 ppb with a maximum value of 432.3 ppb, indicating the strong photochemistry and
569 secondary formation of ozone. Comparing the OFP results in the three clusters,
570 contribution of aromatic and aliphatic HCs decreased from cluster 1 to 3, while that of
571 $C_xH_yO_1$ and $C_xH_yO_2$ increased from 27% and 19% to 40% and 21%, respectively. The
572 top 5 species contributing to OFP were acetaldehyde, butenes, butanedione, C_8
573 aromatics and formaldehyde, which accounted for 13%-16%, 11%-12%, 11%-12%,
574 5%-8%, and 7%-8% of total OFP contributed by all species in the three clusters,
575 respectively (Figure S8). The significant contributions from these 5 species were due
576 to their high reactivity (MIR>6) and relatively high mass concentrations. OVOCs
577 contributed over 50% of OFP in this study, among which $C_xH_yO_1$ was the predominant
578 contributor to OFP. Most of $C_xH_yO_1$ was aldehydes which have high reactivity and thus
579 can generate OH radicals by photolysis and then contribute to ozone (Volkamer et al.,
580 2010). Previous emission inventory studies evaluated more on the primary emission
581 sources, while the secondary sources were less studied (Zheng et al., 2009). The high
582 abundance and reactivity of OVOCs suggests further investigation of the OVOC
583 sources and major precursors are important in mitigating ozone pollution.

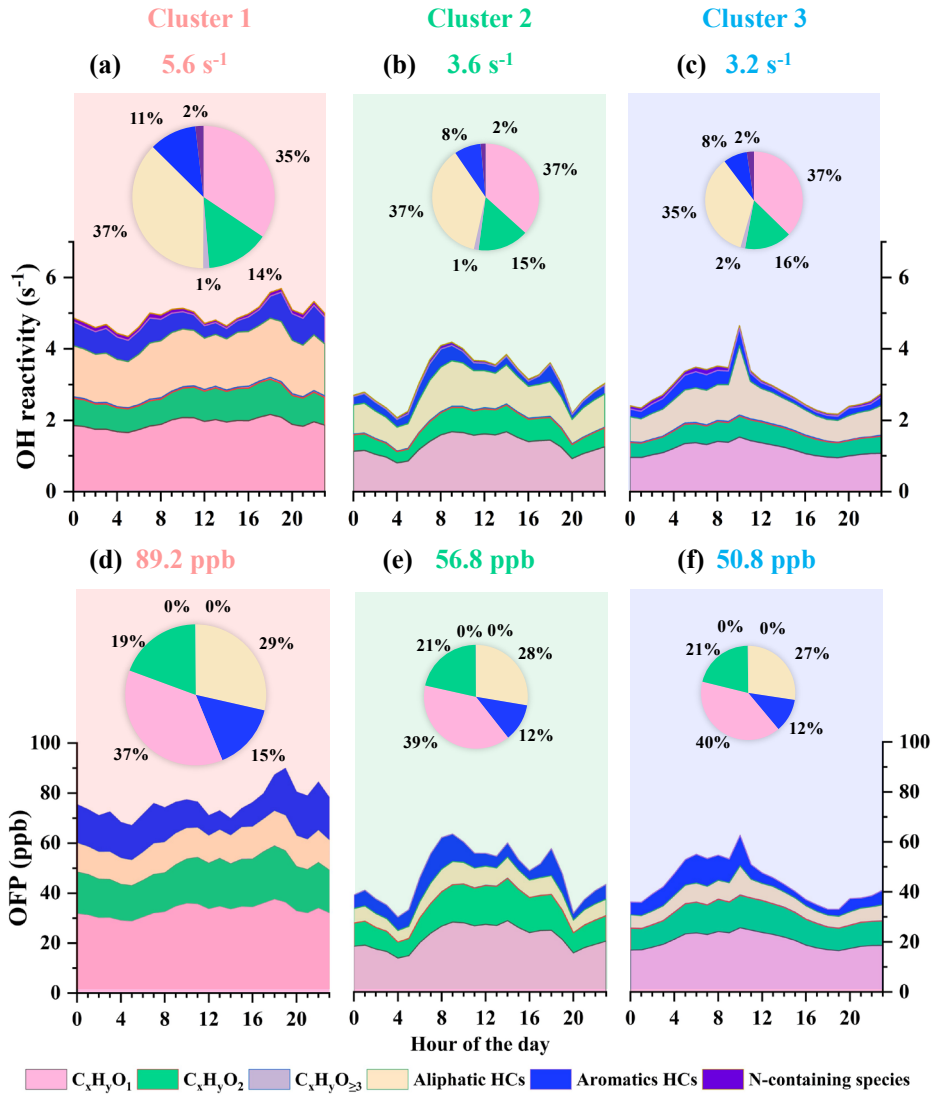

Figure 6. Contribution of classified VOC groups to total OH reactivity and diurnal profiles of OH reactivity in three clusters (a-c), and contribution of classified VOC groups to total OFP and diurnal profiles of OFP in three clusters (d-f).

4. Conclusions

Real-time monitoring of VOCs at a background site in Hong Kong was implemented to improve our understanding of the pollution levels and variabilities, to identify their sources and transformation, as well as to assess the contributions of individual VOCs

and their sources to OH reactivity and OFP. The mixing ratio of VOCs was characterized by high levels of OVOCs, dominated by $C_xH_yO_1$ (53.7%), $C_xH_yO_2$ (23.9%) and $C_xH_yO_{\geq 3}$ (4.6%). The top five species were methanol (4.63 ± 2.47 ppb), acetone (3.37 ± 1.55 ppb), acetic acid (2.51 ± 1.58 ppb), acetaldehyde (1.72 ± 0.88 ppb), formaldehyde (0.93 ± 0.39 ppb). Compared with other background and rural sites, higher levels of OVOCs and lower levels of HCs suggested that transportation and atmospheric oxidation of anthropogenic VOCs may contribute a certain amount of OVOCs at Hok Tsui. Moreover, varied degrees of the ageing of air masses from different source regions and transportation distance were confirmed with paired HCs with their corresponding oxygenated products. PMF results further highlighted primary emissions from anthropogenic sources (vehicle, industrial, solvent usage and primary OVOC sources) and secondary OVOCs comprised the dominant sources, both contributing over 40% of the total analyzed VOC. According to the cluster analysis and PMF results, ambient VOCs were more likely influenced by anthropogenic emissions from inland and coastal eastern China, resulting in aged air masses arriving Hong Kong. OVOCs contributed to over 50% of total OH reactivity and OFP, with the highest contribution from acetaldehyde in all three clusters. The high levels of total OH reactivity and OFP in Cluster 1 (ave. 5.6 s^{-1} and 89.2 ppb) and relatively higher proportions of OVOCs in Cluster 2 (3.6 s^{-1} and 56.8 ppb) and 3 (3.2 s^{-1} and 50.8 ppb) indicate varied impacts of air masses from different regions. More specifically, short-range transportation of air masses from the PRD and southeastern China brought high levels of primary VOCs, while the longer-range transport of air masses from eastern

and northern China brought aged pollutants with high reactivity and potential to form O_3. These results highlight that the significant variation of pollution characteristics of VOCs in the transport and chemical oxidation processes in different air masses have significant impact on the atmospheric oxidation capacity. Jointly controlling strategies should be made case by case and region to region aiming at solving pollution problems from different regions.

Acknowledgements

The authors thank Mr. Steven Poon for his contribution to the field study. This research was financially supported by the Research Grants Council (RGC) of Hong Kong Special Administrative Region, China (Project No. T24-504/17-N, T31-603/21-N, and PolyU 15211522), the Environment and Conservation Fund (Project No. ECF63/2019), and Green Tech Fund (GTF202110151). The authors would like to acknowledge the HKPolyU University Research Facility in Chemical and Environmental Analysis (UCEA) for the equipment support, and Hong Kong Environmental Protection Department for providing access to the Cape D' Aguilar Supersite AQMS and for sharing the trace gases and meteorological data at the supersite.

Reference

Abdullahi, K. L., Delgado-Saborit, J. M., and Harrison, R. M., 2013. Emissions and indoor concentrations of particulate matter and its specific chemical components from cooking: A review, Atmos. Environ., 71, 260-294, https://doi.org/10.1016/j.atmosenv.2013.01.061.

Atkinson, R., 2000. Atmospheric chemistry of VOCs and NO_x, Atmos. Environ., 34, 2063-2101, https://doi.org/10.1016/S1352-2310(99)00460-4.

Atkinson, R., and Arey, J., 2003. Atmospheric degradation of volatile organic compounds, Chem. Rev., 103, 4605-4638, https://10.1021/cr0206420.

Atkinson, R., Baulch, D. L., Cox, R. A., Crowley, J. N., Hampson, R. F., Hynes, R. G., Jenkin, M. E., Rossi, M. J., Troe, J., and Subcommittee, I., 2006. Evaluated kinetic and photochemical data for atmospheric chemistry: Volume II - gas phase reactions of organic species, Atmos. Chem. Phys., 6, 3625-4055, https://10.5194/acp-6-3625-2006.

Barnes, I., Solignac, G., Mellouki, A., and Becker, K. H., 2010. Aspects of the atmospheric chemistry of amides, ChemPhysChem, 11, 3844-3857, https://doi.org/10.1002/cphc.201000374.

Baudic, A., Gros, V., Sauvage, S., Locoge, N., Sanchez, O., Sarda-Estève, R., Kalogridis, C., Petit, J. E., Bonnaire, N., Baisnée, D., Favez, O., Albinet, A., Sciare, J., and Bonsang, B., 2016. Seasonal variability and source apportionment of volatile organic compounds (VOCs) in the Paris megacity (France), Atmospheric Chemistry and Physics, 16, 11961-11989, https://10.5194/acp-16-11961-2016.

Borbon, A., Fontaine, H., Veillerot, M., Locoge, N., Galloo, J. C., and Guillermo, R., 2001. An investigation into the traffic-related fraction of isoprene at an urban location, Atmospheric Environment, 35, 3749-3760, https://doi.org/10.1016/S1352-2310(01)00170-4.

Borbon, A., Gilman, J. B., Kuster, W. C., Grand, N., Chevaillier, S., Colomb, A., Dolgorouky, C., Gros, V., Lopez, M., Sarda-Esteve, R., Holloway, J., Stutz, J., Petetin, H., McKeen, S., Beekmann, M., Warneke, C., Parrish, D. D., and de Gouw, J. A., 2013. Emission ratios of anthropogenic volatile organic compounds in northern mid-latitude megacities: Observations versus emission inventories in Los Angeles and Paris, Journal of Geophysical Research Atmosphere, 118, 2041-2057, https://doi.org/10.1002/jgrd.50059.

Calvert, J., Mellouki, A., Orlando, J., Pilling, M., and Wallington, T., 2011. Mechanisms of atmospheric oxidation of the oxygenates, Oxford University Press

Calvert, J. G., Atkinson, R., Becker, K. H., Kamens, R. M., Wallington, T. H., Seinfeld, J. H., and Yarwood, G., 2002. The Mechanisms of Atmospheric Oxidation of Aromatic Hydrocarbons, Oxford University Press

Canonaco, F., Crippa, M., Slowik, J. G., Baltensperger, U., and Prévôt, A. S. H., 2013. SoFi, an IGOR-based interface for the efficient use of the generalized multilinear engine (ME-2) for the source apportionment: ME-2 application to aerosol mass spectrometer data, Atmospheric Measurement Techniques, 6, 3649-3661, https://10.5194/amt-6-3649-2013.

Cao, T., Wang, H., Li, L., Lu, X., Liu, Y., and Fan, S., 2024. Fast spreading of surface ozone in both temporal and spatial scale in Pearl River Delta, Journal of Environmental Sciences, 137, 540-552, https://doi.org/10.1016/j.jes.2023.02.025.

Carter, W. P. L., 1994. Development of ozone reactivity scales for volatile organic compounds, J. Air Waste Manag. Assoc., 44, 881-899, https://10.1080/1073161X.1994.10467290.

Chen, Y., Yang, Y., and Gao, M., 2023. Typhoon-associated air quality over the Guangdong–Hong Kong–

Macao Greater Bay Area, China: machine-learning-based prediction and assessment, Atmos. Meas. Tech., 16, 1279-1294, 10.5194/amt-16-1279-2023.

Cui, L., Li, H. W., Huang, Y., Zhang, Z., Lee, S. C., Blake, D. R., Wang, X. M., Ho, K. F., and Cao, J. J., 2021. The characteristics and sources of roadside VOCs in Hong Kong: Effect of the LPG catalytic converter replacement programme, Sci. Total Environ., 757, 143811, https://doi.org/10.1016/j.scitotenv.2020.143811.

de Gouw, J. A., Warneke, C., Parrish, D. D., Holloway, J. S., Trainer, M., and Fehsenfeld, F. C., 2003. Emission sources and ocean uptake of acetonitrile (CH_3CN) in the atmosphere, 108, https://doi.org/10.1029/2002JD002897.

Debevec, C., Sauvage, S., Gros, V., Sciare, J., Pikridas, M., Stavroulas, I., Salameh, T., Leonardis, T., Gaudion, V., Depelchin, L., Fronval, I., Sarda-Esteve, R., Baisnée, D., Bonsang, B., Savvides, C., Vrekoussis, M., and Locoge, N., 2017. Origin and variability in volatile organic compounds observed at an Eastern Mediterranean background site (Cyprus), Atmospheric Chemistry and Physics, 17, 11355-11388, https://10.5194/acp-17-11355-2017.

Fall, R., 1999. Chapter 2 - Biogenic emissions of volatile organic compounds from higher plants, in: Reactive hydrocarbons in the atmosphere, edited by: Hewitt, C. N., Academic Press, San Diego, 41-96, https://doi.org/10.1016/B978-012346240-4/50003-5.

Fischer, E. V., Jacob, D. J., Yantosca, R. M., Sulprizio, M. P., Millet, D. B., Mao, J., Paulot, F., Singh, H. B., Roiger, A., Ries, L., Talbot, R. W., Dzepina, K., and Pandey Deolal, S., 2014. Atmospheric peroxyacetyl nitrate (PAN): a global budget and source attribution, Atmospheric Chemistry and Physics, 14, 2679-2698, https://10.5194/acp-14-2679-2014.

Fortems-Cheiney, A., Chevallier, F., Pison, I., Bousquet, P., Saunois, M., Szopa, S., Cressot, C., Kurosu, T. P., Chance, K., and Fried, A., 2012. The formaldehyde budget as seen by a global-scale multi-constraint and multi-species inversion system, Atmospheric Chemistry and Physics, 12, 6699-6721, https://10.5194/acp-12-6699-2012.

Gery, M. W., Fox, D. L., Jeffries, H. E., Stockburger, L., and Weathers, W. S., 1985. A continuous stirred tank reactor investigation of the gas-phase reaction of hydroxyl radicals and toluene, Int. J. Chem. Kinet., 17, 931-955, https://doi.org/10.1002/kin.550170903.

Guenther, A., Hewitt, C. N., Erickson, D., Fall, R., Geron, C., Graedel, T., Harley, P., Klinger, L., Lerdau, M., McKay, W. A., Pierce, T., Scholes, B., Steinbrecher, R., Tallamraju, R., Taylor, J., and Zimmerman, P., 1995. A global model of natural volatile organic compound emissions, Journal of Geophysical Research Atmosphere, 100, 8873-8892, https://l10.1029/94jd02950.

Han, C., Liu, R., Luo, H., Li, G., Ma, S., Chen, J., and An, T., 2019a. Pollution profiles of volatile organic compounds from different urban functional areas in Guangzhou China based on GC/MS and PTR-TOF-MS: Atmospheric environmental implications, Atmos. Environ., 214, 116843, https://doi.org/10.1016/j.atmosenv.2019.116843.

Han, S., Tan, Y., Gao, Y., Li, X., Ho, S. S. H., Wang, M., and Lee, S.-c., 2023. Volatile organic compounds at a roadside site in Hong Kong: Characteristics, chemical reactivity, and health risk assessment, Sci. Total Environ., 866, 161370, https://doi.org/10.1016/j.scitotenv.2022.161370.

Han, Y., Huang, X., Wang, C., Zhu, B., and He, L., 2019b. Characterizing oxygenated volatile organic compounds and their sources in rural atmospheres in China, J. Environ. Sci., 81, 148-155, https://doi.org/10.1016/j.jes.2019.01.017.

He, K., Shen, Z., Zhang, B., Sun, J., Zou, H., Zhou, M., Zhang, Z., Xu, H., Ho, S. S. H., and Cao, J., 2022. Emission profiles of volatile organic compounds from various geological maturity coal

and its clean coal briquetting in China, Atmos. Res., 274, 106200, https://doi.org/10.1016/j.atmosres.2022.106200.

He, K., Fu, T., Zhang, B., Xu, H., Sun, J., Zou, H., Zhang, Z., Hang Ho, S. S., Cao, J., and Shen, Z., 2023. Examination of long-time aging process on volatile organic compounds emitted from solid fuel combustion in a rural area of China, Chemosphere, 333, 138957, https://doi.org/10.1016/j.chemosphere.2023.138957.

Hong-li, W., Sheng-ao, J., Sheng-rong, L., Qing-yao, H., Li, L., Shi-kang, T., Cheng, H., Li-ping, Q., and Chang-hong, C., 2017. Volatile organic compounds (VOCs) source profiles of on-road vehicle emissions in China, Sci. Total Environ., 607-608, 253-261, https://doi.org/10.1016/j.scitotenv.2017.07.001.

Huang, H., Wang, Z., Dai, C., Wu, H., Guo, J., Wang, C., and Zhang, X., 2024. Species profile and reactivity of volatile organic compounds emission in solvent uses, industry activities and from vehicular tunnels, J. Environ. Sci., 135, 546-559, https://doi.org/10.1016/j.jes.2022.08.035.

Huang, X.-F., Wang, C., Zhu, B., Lin, L.-L., and He, L.-Y., 2019. Exploration of sources of OVOCs in various atmospheres in southern China, Environ. Pollut., 249, 831-842, https://doi.org/10.1016/j.envpol.2019.03.106.

Huang, X.-F., Zhang, B., Xia, S.-Y., Han, Y., Wang, C., Yu, G.-H., and Feng, N., 2020. Sources of oxygenated volatile organic compounds (OVOCs) in urban atmospheres in North and South China, Environ. Pollut., 261, 114152, https://doi.org/10.1016/j.envpol.2020.114152.

Huang, Y., Ling, Z. H., Lee, S. C., Ho, S. S. H., Cao, J. J., Blake, D. R., Cheng, Y., Lai, S. C., Ho, K. F., Gao, Y., Cui, L., and Louie, P. K. K., 2015. Characterization of volatile organic compounds at a roadside environment in Hong Kong: An investigation of influences after air pollution control strategies, Atmos. Environ., 122, 809-818, https://doi.org/10.1016/j.atmosenv.2015.09.036.

Jerrett, M., Burnett, R. T., Pope, C. A., 3rd, Ito, K., Thurston, G., Krewski, D., Shi, Y., Calle, E., and Thun, M., 2009. Long-term ozone exposure and mortality, The New England journal of medicine, 360, 1085-1095, https://l10.1056/NEJMoa0803894.

Jordan, C., Fitz, E., Hagan, T., Sive, B., Frinak, E., Haase, K., Cottrell, L., Buckley, S., and Talbot, R., 2009. Long-term study of VOCs measured with PTR-MS at a rural site in New Hampshire with urban influences, Atmospheric Chemistry and Physics, 9, 4677-4697, https://10.5194/acp-9-4677-2009.

Khan, M. A. H., Cooke, M. C., Utembe, S. R., Archibald, A. T., Maxwell, P., Morris, W. C., Xiao, P., Derwent, R. G., Jenkin, M. E., Percival, C. J., Walsh, R. C., Young, T. D. S., Simmonds, P. G., Nickless, G., O'Doherty, S., and Shallcross, D. E., 2015. A study of global atmospheric budget and distribution of acetone using global atmospheric model STOCHEM-CRI, Atmos. Environ., 112, 269-277, https://doi.org/10.1016/j.atmosenv.2015.04.056.

Legreid, G., Lööv, J. B., Staehelin, J., Hueglin, C., Hill, M., Buchmann, B., Prevot, A. S. H., and Reimann, S., 2007. Oxygenated volatile organic compounds (OVOCs) at an urban background site in Zürich (Europe): Seasonal variation and source allocation, Atmos. Environ., 41, 8409-8423, https://doi.org/10.1016/j.atmosenv.2007.07.026.

Li, L., and Wang, X., 2012. Seasonal and diurnal variations of atmospheric non-methane hydrocarbons in Guangzhou, China, International journal of environmental research and public health, 9, 1859-1873, https://l10.3390/ijerph9051859.

Li, X. B., Yuan, B., Wang, S., Wang, C., Lan, J., Liu, Z., Song, Y., He, X., Huangfu, Y., Pei, C., Cheng, P., Yang, S., Qi, J., Wu, C., Huang, S., You, Y., Chang, M., Zheng, H., Yang, W., Wang, X., and

765 Shao, M., 2022. Variations and sources of volatile organic compounds (VOCs) in urban region:
766 insights from measurements on a tall tower, Atmospheric Chemistry and Physics, 22, 10567-
767 10587, https://l10.5194/acp-22-10567-2022.
768 Li, Z., Xue, L., Yang, X., Zha, Q., Tham, Y. J., Yan, C., Louie, P. K. K., Luk, C. W. Y., Wang, T., and
769 Wang, W., 2018. Oxidizing capacity of the rural atmosphere in Hong Kong, Southern China,
770 Sci. Total Environ., 612, 1114-1122, https://doi.org/10.1016/j.scitotenv.2017.08.310.
771 Liang, X., Chen, X., Zhang, J., Shi, T., Sun, X., Fan, L., Wang, L., and Ye, D., 2017. Reactivity-based
772 industrial volatile organic compounds emission inventory and its implications for ozone control
773 strategies in China, Atmos. Environ., 162, 115-126,
774 https://doi.org/10.1016/j.atmosenv.2017.04.036.
775 Liu, Y., Yuan, B., Li, X., Shao, M., Lu, S., Li, Y., Chang, C. C., Wang, Z., Hu, W., Huang, X., He, L.,
776 Zeng, L., Hu, M., and Zhu, T., 2015. Impact of pollution controls in Beijing on atmospheric
777 oxygenated volatile organic compounds (OVOCs) during the 2008 Olympic Games:
778 observation and modeling implications, Atmospheric Chemistry and Physics, 15, 3045-3062,
779 https://l10.5194/acp-15-3045-2015.
780 Löfgren, L., and Petersson, G., 1992. Butenes and butadiene in urban air, Sci. Total Environ., 116, 195-
781 201, https://doi.org/10.1016/0048-9697(92)90374-2.
782 McKeen, S. A., and Liu, S. C., 1993. Hydrocarbon ratios and photochemical history of air masses,
783 Geophys. Res. Lett., 20, 2363-2366, https://doi.org/10.1029/93GL02527.
784 McKeen, S. A., Liu, S. C., Hsie, E.-Y., Lin, X., Bradshaw, J. D., Smyth, S., Gregory, G. L., and Blake,
785 D. R., 1996. Hydrocarbon ratios during PEM-WEST A: A model perspective, Journal of
786 Geophysical Research Atmosphere, 101, 2087-2109, https://doi.org/10.1029/95JD02733.
787 Millet, D. B., Guenther, A., Siegel, D. A., Nelson, N. B., Singh, H. B., de Gouw, J. A., Warneke, C.,
788 Williams, J., Eerdekens, G., Sinha, V., Karl, T., Flocke, F., Apel, E., Riemer, D. D., Palmer, P.
789 I., and Barkley, M., 2010. Global atmospheric budget of acetaldehyde: 3-D model analysis and
790 constraints from in-situ and satellite observations, Atmospheric Chemistry and Physics, 10,
791 3405-3425, https://l10.5194/acp-10-3405-2010.
792 Mo, Z., Shao, M., and Lu, S., 2016. Compilation of a source profile database for hydrocarbon and OVOC
793 emissions in China, Atmos. Environ., 143, 209-217,
794 https://doi.org/10.1016/j.atmosenv.2016.08.025.
795 Mohd Hanif, N., Limi Hawari, N. S. S., Othman, M., Abd Hamid, H. H., Ahamad, F., Uning, R., Ooi, M.
796 C. G., Wahab, M. I. A., Sahani, M., and Latif, M. T., 2021. Ambient volatile organic compounds
797 in tropical environments: Potential sources, composition and impacts – A review, Chemosphere
798 (Oxford), 285, 131355-131355, https://l10.1016/j.chemosphere.2021.131355.
799 Moore, D. P., Remedios, J. J., and Waterfall, A. M., 2012. Global distributions of acetone in the upper
800 troposphere from MIPAS spectra, Atmospheric Chemistry and Physics, 12, 757-768,
801 https://l10.5194/acp-12-757-2012.
802 Nelson, P. F., and Quigley, S. M., 1984. The hydrocarbon composition of exhaust emitted from gasoline
803 fuelled vehicles, Atmos. Environ., 18, 79-87, https://doi.org/10.1016/0004-6981(84)90230-0.
804 Ou, J., Zheng, J., Li, R., Huang, X., Zhong, Z., Zhong, L., and Lin, H., 2015. Speciated OVOC and VOC
805 emission inventories and their implications for reactivity-based ozone control strategy in the
806 Pearl River Delta region, China, Sci. Total Environ., 530-531, 393-402,
807 https://doi.org/10.1016/j.scitotenv.2015.05.062.
808 Paatero, P., 1999. The multilinear engine—a table-driven, least squares program for solving multilinear

problems, including the n-way parallel factor analysis model, J. Comput. Graph. Stat., 8, 854-888, https://l10.1080/10618600.1999.10474853.

Paulot, F., Wunch, D., Crounse, J. D., Toon, G. C., Millet, D. B., DeCarlo, P. F., Vigouroux, C., Deutscher, N. M., González Abad, G., Notholt, J., Warneke, T., Hannigan, J. W., Warneke, C., de Gouw, J. A., Dunlea, E. J., De Mazière, M., Griffith, D. W. T., Bernath, P., Jimenez, J. L., and Wennberg, P. O., 2011. Importance of secondary sources in the atmospheric budgets of formic and acetic acids, Atmos. Chem. Phys., 11, 1989-2013, 10.5194/acp-11-1989-2011.

Placet, M., Mann, C. O., Gilbert, R. O., and Niefer, M. J., 2000. Emissions of ozone precursors from stationary sources:: a critical review, Atmos. Environ., 34, 2183-2204, https://doi.org/10.1016/S1352-2310(99)00464-1.

Prévôt, A. S. H., Dommen, J., Bäumle, M., and Furger, M., 2000. Diurnal variations of volatile organic compounds and local circulation systems in an Alpine valley, Atmos. Environ., 34, 1413-1423, https://doi.org/10.1016/S1352-2310(99)00440-9.

Salvador, C. M. G., Tang, R., Priestley, M., Li, L., Tsiligiannis, E., Le Breton, M., Zhu, W., Zeng, L., Wang, H., Yu, Y., Hu, M., Guo, S., and Hallquist, M., 2021. Ambient nitro-aromatic compounds – biomass burning versus secondary formation in rural China, Atmospheric Chemistry and Physics, 21, 1389-1406, https://l10.5194/acp-21-1389-2021.

Sawyer, R. F., Harley, R. A., Cadle, S. H., Norbeck, J. M., Slott, R., and Bravo, H. A., 2000. Mobile sources critical review: 1998 NARSTO assessment, Atmos. Environ., 34, 2161-2181, https://doi.org/10.1016/S1352-2310(99)00463-X.

Seinfeld, J. H., and Pandis, S. N., 2016. Atmospheric Chemistry and Physics: From Air Pollution to Climate Change, 3 ed., Wiley, New York

Shao, P., Xu, X., Zhang, X., Xu, J., Wang, Y., and Ma, Z., 2020. Impact of volatile organic compounds and photochemical activities on particulate matters during a high ozone episode at urban, suburb and regional background stations in Beijing, Atmos. Environ., 236, 117629, https://doi.org/10.1016/j.atmosenv.2020.117629.

Simon, H., Beck, L., Bhave, P. V., Divita, F., Hsu, Y., Luecken, D., Mobley, J. D., Pouliot, G. A., Reff, A., Sarwar, G., and Strum, M., 2010. The development and uses of EPA's SPECIATE database, Atmos. Pollut. Res., 1, 196-206, https://doi.org/10.5094/APR.2010.026.

Singh, H. B., O'Hara, D., Herlth, D., Sachse, W., Blake, D. R., Bradshaw, J. D., Kanakidou, M., and Crutzen, P. J., 1994. Acetone in the atmosphere: Distribution, sources, and sinks, Journal of Geophysical Research Atmosphere, 99, 1805-1819, https://doi.org/10.1029/93JD00764.

Singh, H. B., Salas, L., Herlth, D., Kolyer, R., Czech, E., Viezee, W., Li, Q., Jacob, D. J., Blake, D., Sachse, G., Harward, C. N., Fuelberg, H., Kiley, C. M., Zhao, Y., and Kondo, Y., 2003. In situ measurements of HCN and CH3CN over the Pacific Ocean: Sources, sinks, and budgets, Journal of Geophysical Research Atmosphere, 108, https://doi.org/10.1029/2002JD003006.

Singsaas, E. L., and Sharkey, T. D., 1998. The regulation of isoprene emission responses to rapid leaf temperature fluctuations, Plant Cell Environ., 21, 1181-1188, https://doi.org/10.1046/j.1365-3040.1998.00380.x.

St Helen, G., Jacob, P., 3rd, Peng, M., Dempsey, D. A., Hammond, S. K., and Benowitz, N. L., 2014. Intake of toxic and carcinogenic volatile organic compounds from secondhand smoke in motor vehicles, Cancer epidemiology, biomarkers & prevention : a publication of the American Association for Cancer Research, cosponsored by the American Society of Preventive Oncology, 23, 2774-2782, https://10.1158/1055-9965.Epi-14-0548.

Sun, J., Shen, Z., Wang, R., Li, G., Zhang, Y., Zhang, B., He, K., Tang, Z., Xu, H., Qu, L., Sai Hang Ho, S., Liu, S., and Cao, J., 2021. A comprehensive study on ozone pollution in a megacity in North China Plain during summertime: Observations, source attributions and ozone sensitivity, Environ. Int., 146, 106279, https://doi.org/10.1016/j.envint.2020.106279.

Tan, Y., Han, S., Chen, Y., Zhang, Z., Li, H., Li, W., Yuan, Q., Li, X., Wang, T., and Lee, S.-c., 2021. Characteristics and source apportionment of volatile organic compounds (VOCs) at a coastal site in Hong Kong, Sci. Total Environ., 777, 146241, https://doi.org/10.1016/j.scitotenv.2021.146241.

Tingey, D. T., Marybeth, M., Grothaus, L. C., and Burns, W. F., 1980. Influence of light and temperature on monoterpene emission rates from slash pine, Plant Physiol., 65, 797-801, https://10.1104/pp.65.5.797.

Tsui, J. K.-Y., Guenther, A., Yip, W.-K., and Chen, F., 2009. A biogenic volatile organic compound emission inventory for Hong Kong, Atmospheric Environment, 43, 6442-6448, https://doi.org/10.1016/j.atmosenv.2008.01.027.

Volkamer, R., Sheehy, P., Molina, L. T., and Molina, M. J., 2010. Oxidative capacity of the Mexico City atmosphere – Part 1: A radical source perspective, Atmospheric Chemistry and Physics, 10, 6969-6991, https://10.5194/acp-10-6969-2010.

Wang, H., Wang, Q., Chen, J., Chen, C., Huang, C., Qiao, L., Lou, S., and Lu, J., 2015. Do vehicular emissions dominate the source of C_6–C_8 aromatics in the megacity Shanghai of eastern China?, J. Environ. Sci., 27, 290-297, https://doi.org/10.1016/j.jes.2014.05.033.

Wang, Y. Q., Zhang, X. Y., and Draxler, R. R., 2009. TrajStat: GIS-based software that uses various trajectory statistical analysis methods to identify potential sources from long-term air pollution measurement data, Environ. Model. Softw., 24, 938-939, https://doi.org/10.1016/j.envsoft.2009.01.004.

Wei, W., Wang, S., Hao, J., and Cheng, S., 2011. Projection of anthropogenic volatile organic compounds (VOCs) emissions in China for the period 2010–2020, Atmospheric environment (1994), 45, 6863-6871, https://10.1016/j.atmosenv.2011.01.013.

Xu, Y., Yan, Y., Duan, X., Peng, L., Wu, J., Zhang, X., Niu, Y., Liu, Z., Zhang, D., and Wei, X., 2022. Diurnal variation and source analysis of NMHCs at a background site of Nam Co (4,730 m a.s.l.) in the interior area of Tibetan Plateau, Atmos. Pollut. Res., 13, 101520, https://doi.org/10.1016/j.apr.2022.101520.

Xu, Z., Wang, T., Xue, L. K., Louie, P. K. K., Luk, C. W. Y., Gao, J., Wang, S. L., Chai, F. H., and Wang, W. X., 2013. Evaluating the uncertainties of thermal catalytic conversion in measuring atmospheric nitrogen dioxide at four differently polluted sites in China, Atmos. Environ., 76, 221-226, https://doi.org/10.1016/j.atmosenv.2012.09.043.

Xue, L., Gu, R., Wang, T., Wang, X., Saunders, S., Blake, D., Louie, P. K. K., Luk, C. W. Y., Simpson, I., Xu, Z., Wang, Z., Gao, Y., Lee, S., Mellouki, A., and Wang, W., 2016. Oxidative capacity and radical chemistry in the polluted atmosphere of Hong Kong and Pearl River Delta region: analysis of a severe photochemical smog episode, Atmospheric Chemistry and Physics, 16, 9891-9903, https://10.5194/acp-16-9891-2016.

Xue, L. K., Wang, T., Guo, H., Blake, D. R., Tang, J., Zhang, X. C., Saunders, S. M., and Wang, W. X., 2013. Sources and photochemistry of volatile organic compounds in the remote atmosphere of western China: results from the Mt. Waliguan Observatory, Atmospheric Chemistry and Physics, 13, 8551-8567, https://10.5194/acp-13-8551-2013.

Yang, D., Li, C., Lau, A. K.-H., and Li, Y., 2013. Long-term measurement of daytime atmospheric mixing layer height over Hong Kong, Journal of Geophysical Research: Atmosphere, 118, 2422-2433, https://doi.org/10.1002/jgrd.50251.

Yang, M., Li, F., Huang, C., Tong, L., Dai, X., and Xiao, H., 2023. VOC characteristics and their source apportionment in a coastal industrial area in the Yangtze River Delta, China, J. Environ. Sci., 127, 483-494, https://doi.org/10.1016/j.jes.2022.05.041.

Yang, Y., Liu, B., Hua, J., Yang, T., Dai, Q., Wu, J., Feng, Y., and Hopke, P. K., 2022. Global review of source apportionment of volatile organic compounds based on highly time-resolved data from 2015 to 2021, Environ. Int., 165, 107330, https://doi.org/10.1016/j.envint.2022.107330.

Yeoman, A. M., Shaw, M., Carslaw, N., Murrells, T., Passant, N., and Lewis, A. C., 2020. Simplified speciation and atmospheric volatile organic compound emission rates from non - aerosol personal care products, Indoor air, 30, 459-472, https://10.1111/ina.12652.

Yuan, B., Chen, W., Shao, M., Wang, M., Lu, S., Wang, B., Liu, Y., Chang, C.-C., and Wang, B., 2012. Measurements of ambient hydrocarbons and carbonyls in the Pearl River Delta (PRD), China, Atmos. Res., 116, 93-104, https://doi.org/10.1016/j.atmosres.2012.03.006.

Yuan, B., Koss, A. R., Warneke, C., Coggon, M., Sekimoto, K., and de Gouw, J. A., 2017. Proton-transfer-reaction mass spectrometry: Applications in atmospheric sciences, Chem. Rev., 117, 13187-13229, https://10.1021/acs.chemrev.7b00325.

Zhang, H., Chen, C., Yan, W., Wu, N., Bo, Y., Zhang, Q., and He, K., 2021. Characteristics and sources of non-methane VOCs and their roles in SOA formation during autumn in a central Chinese city, Sci. Total Environ., 782, 146802, https://doi.org/10.1016/j.scitotenv.2021.146802.

Zhang, Y., Wang, X., Barletta, B., Simpson, I. J., Blake, D. R., Fu, X., Zhang, Z., He, Q., Liu, T., Zhao, X., and Ding, X., 2013. Source attributions of hazardous aromatic hydrocarbons in urban, suburban and rural areas in the Pearl River Delta (PRD) region, J. Hazard. Mater., 250-251, 403-411, https://doi.org/10.1016/j.jhazmat.2013.02.023.

Zheng, J., Shao, M., Che, W., Zhang, L., Zhong, L., Zhang, Y., Streets, D. J. E. s., and technology, 2009. Speciated VOC emission inventory and spatial patterns of ozone formation potential in the Pearl River Delta, China, Environ. Sci. Technol., 43, 8580-8586, https://doi.org/10.1021/es901688e.

Zhou, X., Li, Z., Zhang, T., Wang, F., Wang, F., Tao, Y., Zhang, X., Wang, F., and Huang, J., 2019. Volatile organic compounds in a typical petrochemical industrialized valley city of northwest China based on high-resolution PTR-MS measurements: Characterization, sources and chemical effects, Science of The Total Environment, 671, 883-896, https://doi.org/10.1016/j.scitotenv.2019.03.283.

Zhu, B., Han, Y., Wang, C., Huang, X., Xia, S., Niu, Y., Yin, Z., and He, L., 2019. Understanding primary and secondary sources of ambient oxygenated volatile organic compounds in Shenzhen utilizing photochemical age-based parameterization method, J. Environ. Sci., 75, 105-114, https://doi.org/10.1016/j.jes.2018.03.008.

Table 1. Comparison of the average mixing ratios of typical VOCs at various background, rural, and urban sites (ppb).

Location, Year	Site description	Methanol	Acetaldehyde	Acetone	MEK	MACR+MVK	Isoprene	Monoterpenes	Benzene	Toluene	C_8 aromatics
[a] Hok Tsui, Hong Kong, China, 2020.10-2020.11, this study	background	4.63	1.72	3.37	0.40	0.14	0.20	0.04	0.30	0.39	0.309
[b] Hok Tsui, Hong Kong, China, 2018.09	background	3.73	0.72	2.43	0.46	0.11	0.47	0.13	0.29	0.25	0.260
[c] Hok Tsui, Hong Kong, China, 2012 autumn	background		0.98	0.68			0.49		0.48	0.48	0.193
[d] Nanling, Guangdong, China 2016.11	background	2.79	1.06	2.09	0.59		0.13		0.34	0.42	
[d] Nan'ao, Guangdong, China 2015.12-2016.1	regional	4.60	1.62	1.80	1.80		0.14		0.71	1.70	
[e] Shangdianzi, Beijing, China, 2011.6	background		4.05	3.45	1.03		0.02		1.10	0.37	0.470
[f] Mt.Waliguan, China 2003.4,5,7-8	background						0.04		0.09	0.18	0.189
[g] Cyprus, Italy, 2015.03	background	2.81	0.44	1.10	0.22	0.03	0.05		0.11	0.05	1.183
[h] Zurich, Swizerland, 2005 autumn	background	1.11	0.45	1.24	0.17	0.04	0.08		0.38	1.28	1.030
[i] Nam Co, China, 2020.8	background						0.07		0.54	0.41	0.058
[j] Yangmeikeng, China, 2016.6-2016.7	rural	3.90	0.73	1.77	0.54						
[k] New Hampshire, U.S.	rural	2.61	0.47	2.01	0.21						
[l] Hong Kong, China, 2011	urban						0.26	0.06	0.91	2.74	1.56
[m] Hong Kong, China, 2013	urban		3.49	9.36	1.39				0.56	1.20	
[n] Hong Kong, China, 2014	urban	3.31	1.74	2.18	0.37	0.21	0.63	0.34	0.28	1.73	0.65
[o] Guangzhou, China, 2020	urban	8.68	2.54	4.39	1.18						
[p] Shenzhen,China, 2016 summer	urban	14.47	1.98	3.78	1.33						
[q] Beijing, China, 2008 summer	urban	14.96	2.72	3.96	1.16						
[r] Beijing, China, 2018.5-2018.6	urban	19.70	2.90	4.16	1.00	0.43	0.69		0.65	1.02	1.34

Notes: Data sources for comparison are retrieved from [a] this study, [b] Tan et al. (2021), [c] Li et al. (2018), [d] Huang et al. (2019), [e] Shao et al. (2020), [f] Xue et al. (2013), [g] Debevec et al. (2017), [h] Legreid et al. (2007), [i] Xu et al. (2022), [j] Han et al. (2019b), [k] Jordan et al. (2009), [l] Huang et al. (2015), [m] Han et al. (2023), [n] Cui et al. (2021), [o] Li et al. (2022), [p] Zhu er al. (2019), [q] Liu et al. (2015), [r] Huang et al. (2020).